Kinetic mix mechanisms in shock-driven inertial confinement fusion implosionsa)

H. G. Rinderknecht, H. Sio, C. K. Li, N. Hoffman, A. B. Zylstra, M. J. Rosenberg, J. A. Frenje, M. Gatu Johnson, F. H. Séguin, R. D. Petrasso, R. Betti, V. Yu Glebov, D. D. Meyerhofer, T. C. Sangster, W. Seka, C. Stoeckl, G. Kagan, K. Molvig, C. Bellei, P. Amendt, O. Landen, J. R. Rygg, V. A. Smalyuk, S. Wilks, A. Greenwood, and A. Nikroo

Citation: Physics of Plasmas (1994-present) **21**, 056311 (2014); doi: 10.1063/1.4876615
View online: http://dx.doi.org/10.1063/1.4876615
View Table of Contents: http://scitation.aip.org/content/aip/journal/pop/21/5?ver=pdfcov
Published by the AIP Publishing

Kinetic mix mechanisms in shock-driven inertial confinement fusion implosions[a)]

H. G. Rinderknecht,[1,b)] H. Sio,[1] C. K. Li,[1] N. Hoffman,[2] A. B. Zylstra,[1] M. J. Rosenberg,[1] J. A. Frenje,[1] M. Gatu Johnson,[1] F. H. Séguin,[1] R. D. Petrasso,[1] R. Betti,[3] V. Yu Glebov,[3] D. D. Meyerhofer,[3] T. C. Sangster,[3] W. Seka,[3] C. Stoeckl,[3] G. Kagan,[2] K. Molvig,[2] C. Bellei,[4] P. Amendt,[4] O. Landen,[4] J. R. Rygg,[4] V. A. Smalyuk,[4] S. Wilks,[4] A. Greenwood,[5] and A. Nikroo[5]

[1]*Plasma Science and Fusion Center, Massachusetts Institute of Technology, Cambridge, Massachusetts 02139, USA*
[2]*Los Alamos National Laboratory, Los Alamos, New Mexico 87545, USA*
[3]*Laboratory for Laser Energetics, University of Rochester, Rochester, New York 14623, USA*
[4]*Lawrence Livermore National Laboratory, Livermore, California 94550, USA*
[5]*General Atomics, San Diego, California 92121, USA*

(Received 22 December 2013; accepted 2 April 2014; published online 19 May 2014)

Shock-driven implosions of thin-shell capsules, or "exploding pushers," generate low-density, high-temperature plasmas in which hydrodynamic instability growth is negligible and kinetic effects can play an important role. Data from implosions of thin deuterated-plastic shells with hydroequivalent D^{3}He gas fills ranging from pure deuterium to pure ^{3}He [H. G. Rinderknecht *et al.*, Phys. Rev. Lett. **112**, 135001 (2014)] were obtained to evaluate non-hydrodynamic fuel-shell mix mechanisms. Simulations of the experiments including reduced ion kinetic models support ion diffusion as an explanation for these data. Several additional kinetic mechanisms are investigated and compared to the data to determine which are important in the experiments. Shock acceleration of shell deuterons is estimated to introduce mix less than or comparable to the amount required to explain the data. Beam-target mechanisms are found to produce yields at most an order of magnitude less than the observations. © *2014 AIP Publishing LLC*. [http://dx.doi.org/10.1063/1.4876615]

I. INTRODUCTION

In Inertial Confinement Fusion (ICF), mix of the fuel and shell material is detrimental to the implosion performance, as the introduction of high-Z elements from the shell into the fusion fuel enhances radiative energy loss, reducing the peak pressure of the fuel and consequently the fusion yield.[1] Hydrodynamic instabilities, such as Rayleigh-Taylor (RT), Kelvin-Helmholtz, and Richtmyer-Meshkov, have been extensively studied in laser-driven implosions and in planar plasmas to quantify the contributions of these mechanisms to mix.[2–7] Non-hydrodynamic mechanisms such as diffusive mass flow[8,9] and shock reflection of charged particles[10] can also lead to ion transport and fuel-shell mix. However, non-hydrodynamic mix mechanisms, which may occur during the shock phase of ignition implosions when the fuel is in a kinetic regime, have not previously been explored experimentally. Low shell-mass "exploding pusher" targets are known to have minimal hydrodynamic instability growth due to negligible deceleration phase convergence, providing an experimental platform to study kinetic mechanisms.[11,12]

Thick deuterated plastic (CD) shells filled with either ^{3}He[13,14] or tritium gas[15–18] have previously been used to study hydrodynamic mix mechanisms during the compression phase of ablatively driven implosions. D^{3}He- or DT-fusion reactions in such experiments are only expected to occur in regions where fuel and shell material have been atomically mixed. Experiments on OMEGA have shown that the shock yield from such ablatively driven implosions is below the measurement threshold, from which it is inferred that negligible fuel-shell mix occurs prior to the shock bang-time.[13,14] This finding was in agreement with the expectations from hydrodynamic mix models, which predict that fuel-shell mix only occurs during the deceleration phase when hydrodynamic instability growth is substantial.

In contrast, a series of kinetic mix experiments performed using thin CD-shells filled with pure ^{3}He demonstrated significant fuel-shell mix prior to the deceleration phase.[19] Hydrodynamic instability growth was shown to be negligible prior to the deceleration phase, which means that a non-hydrodynamic mix mechanism must be invoked to explain the data. Ion diffusion was proposed as one plausible explanation of these results, by generating a thin mix-layer near the fuel-shell interface prior to shock-bang time. Other kinetic effects, such as shock acceleration of light ions in the shell, may also play an important role, and such mechanisms are studied here as possible contributing factors.

The impact of the kinetic processes examined herein, in particular shock acceleration, on hot-spot ignition designs is under investigation. Recent ignition designs include four shocks, which are timed to coalesce near the inside surface of the DT-ice layer, generating a single strong shock that traverses the fill gas.[20] Kinetic fuel-shell mixing associated with shock traversal of the fuel-shell interface may occur in

[a)]Paper GI3 5, Bull. Am. Phys. Soc. **58**, 106 (2013).
[b)]Invited speaker.

ignition experiments.[10] Between shock coalescence and the compression phase, the ignition fuel plasmas are comparable to those produced in exploding pusher implosions. The ignition DT-gas fill is low-density ($\rho = 0.3$ mg/cc) and strongly shocked (M ~ 10–50), comparable to expectations for the kinetic mix experiments ($\rho = 0.49$ mg/cc, M $\gg$ 10). Kinetic physics in the strongly shocked gas is a subject of active investigation, as such processes may modify the initial conditions for compression, influencing the evolution of ignition targets later in time.

This paper is organized as follows: Section II discusses the experimental design of the thin CD-shell mix study, including details ruling out the influence of ablation front instabilities in Sec. II A. Section III presents additional data from the experiments. The nuclear data are analyzed by comparison to simulations including Reduced Ion Kinetic (RIK) models[21] in Sec. IV A. In Sec. IV B, several kinetic mechanisms are investigated to determine to what extent they contribute to the observed results, including in particular shock-acceleration of charged particles in Sec. IV B 1 and beam-target models in Sec. IV B 2. The conclusions are presented in Sec. V.

II. EXPERIMENTAL DESIGN

The experiments were performed at the 60-beam OMEGA laser system.[22] Spherical capsules with a diameter of 860 μm and a 5.1 μm-thick deuterated plastic (CD) wall were filled with various mixtures of deuterium and ^{3}He gas. A constant fuel mass density of 0.49 mg/cc was used for the fills of pure deuterium, pure ^{3}He, and 50:50 atomic D^{3}He, in order to maintain hydroequivalence.[23] This condition maintains equal pressure, temperature and density profile evolution for all implosions, to zeroth order.[24] A 0.1 μm outer layer of Aluminum was deposited on the targets to reduce the permeation rate of the fill gas. Targets were imploded using 1 ns square laser pulses, delivering either 30 kJ of laser energy, or 23 kJ of laser energy with smoothing by spectral dispersion to reduce the high-mode nonuniformities in the wave front.[25] Distributed phase plates were used in all cases to generate a fourth-order super-Gaussian beam profile.[26]

The expected evolution of these implosions is shown in Figure 1, which presents a simulation of the above conditions using the 1D-radiation-hydrodynamic code HYADES.[27] A predicted x-ray preheat of the CD-shell to 20 eV was included in these simulations, which has the effect of causing the CD material to blow down by ~20 μm prior to shock breakout at ~250 ps. These thin-shelled "exploding pusher" capsules produce nuclear yield, called "shock yield," primarily from heating of the fuel by the shock during its rebound from the center of the implosion at approximately 0.7 ns. In thick-shelled implosions with substantial remaining shell mass, shock-bang time is immediately followed by the deceleration phase and shell compression of the fuel. The remaining shell material can significantly compress the fuel and generate a second period of nuclear yield production, termed "compression yield." However in these experiments, the CD-shell has burned through prior to deceleration at approximately 0.5 ns, and the remaining CD plasma density is roughly comparable to the fuel plasma density. The effects of this can be seen in the trajectory of the fuel-shell interface after the shock rebound, when the remaining mass is too small to significantly compress and heat the fuel. Little compression yield is expected.

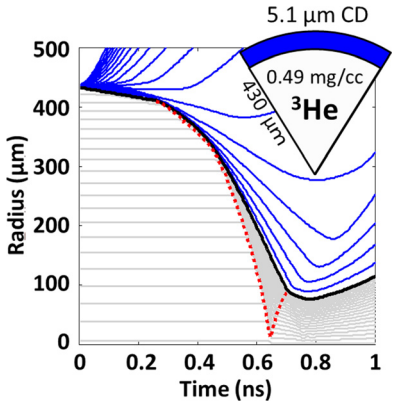

FIG. 1. Lagrangian mass element profiles simulated for a 30-kJ implosion of a 5.1 μm CD shell (blue) filled with 0.49 mg/cc pure ^{3}He (grey). The 1D-radiation-hydrodynamic code HYADES was used for this simulation. The inward trajectory of the fuel-shell interface (black) is interrupted by the rebounding shock (red dotted), initiating a brief deceleration phase. Shock burn occurs when the rebounding shock locally heats and compresses the fuel to fusion-relevant conditions.

A. Ablation front stability

The impact of hydrodynamic instabilities on these targets, including RT instability seeded by laser imprint, Richtmyer-Meshkov instability at the fuel-shell interface, and RT instability during the deceleration phase has been shown to be negligible.[19] The RT instability growth at the ablation front early in time seeded by initial capsule surface roughness was also studied and found not to significantly impact the implosions. Initial surface mode amplitudes were measured by Atomic-Force Microscopy (AFM). The RMS peak amplitude of the initial surface roughness is 0.56 μm, including modes $\ell = 2$ to 1000. This value is dominated by low-order modes: the RMS amplitude is reduced to 0.15 μm for modes $\ell > 5$. Simulated 1D profiles were used to determine the time-dependent Atwood number $\mathcal{A} = (\rho_h - \rho_l)/(\rho_h + \rho_l)$ and local acceleration a. For each timestep in these simulations, the unstable region was identified using the general instability condition $\nabla P \cdot \nabla \rho < 0$,[28] and the maximum growth rate for each mode $\gamma(t, \ell) = \sqrt{\mathcal{A}(t) a(t) k(\ell)}$ was determined, where k(ℓ) is the wavenumber of the mode. Using the measured power spectrum and simulated peak growth rate at each time step, the expected amplitude at time t for modes up to 1000 was estimated as the initial amplitude multiplied by the growth factor $\prod_0^t \exp[\gamma(t_i)\Delta t_i]$. The peak mode amplitudes at burn-through are shown in Figure 2, at which time they reach a maximum RMS of 0.69 μm. Modes above $\ell \approx 300$ have exceeded the regime of linear growth as defined by the Haan saturation criterion.[29] Assuming full atomic fuel-shell mixing, this amplitude is an order of magnitude smaller than the approximately 10 μm mix layer that was shown to be necessary to explain the data.[19] Central to this discussion is that this

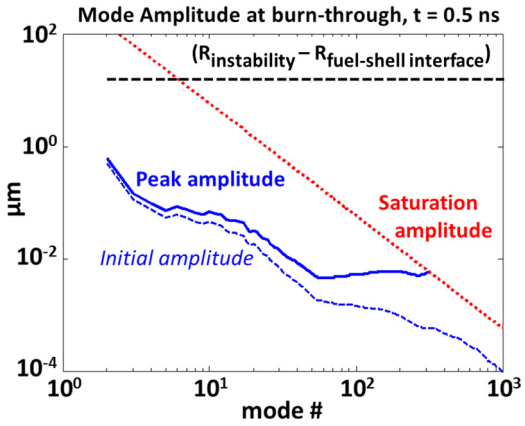

FIG. 2. The expected amplitude of perturbations at the ablation front at shell burn-through ($t \approx 0.5$ ns) as estimated from 1D-simulations. Atomic-force microscopy measurements of the capsule roughness were used for initial amplitudes (blue dashed). At burn-through, all non-saturated modes (blue solid) are at least an order of magnitude smaller than the distance between the region of peak instability and the fuel-shell interface (black dashed). Modes above $\ell \sim 300$ reach the saturation amplitude (red dotted).

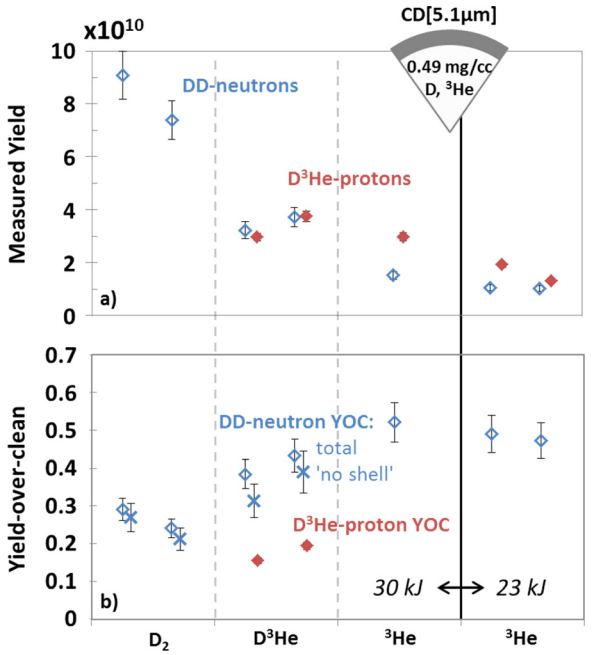

FIG. 3. (a) Nuclear yields of D^3He-protons (solid diamonds, red) and DD-neutrons (open diamonds, blue) from implosions of deuterated plastic shells filled with hydroequivalent mixtures of D_2 (2 shots), D^3He (2 shots) or ^3He gas (1 shot at 30 kJ, 2 shots at 23 kJ). Experiments performed at 30 kJ and 23 kJ showed similar levels of mix as inferred from D^3He-proton yields. (b) YOC compared to 1D-HYADES simulations. DD-neutron YOC is shown for both total yield (open diamonds, blue) and corrected to remove the shell yield contribution (x, blue). The correction assumes that the experimental shell yield is the same for all experiments with the same laser power, as in the simulations.

treatment overestimates the expected growth, as it does not account for the stabilizing effect of the ablation velocity.[4] This analysis reaffirms the previous finding that hydrodynamic instability growth is not sufficient to explain the high levels of mix observed in these experiments.

III. EXPERIMENTAL RESULTS

The yields of 14.7 MeV protons from the D-^{3}He fusion reaction were measured using multiple Wedge-Range-Filter (WRF) proton spectrometers and the Charged Particle Spectrometers (CPS1 and CPS2).[30] D^3He-proton yields above 10^{10} were produced both by capsules containing 50:50 D-^{3}He mixtures and by capsules containing pure ^{3}He. The measured nuclear yields from the D-D fusion reaction were also above 10^{10}, using the neutron Time-of-Flight (nTOF) diagnostic suite for neutrons[31] and CPS1 and CPS2 for the charged particles. A nuclear bang time of 780 ± 50 ps was recorded on one of the hydroequivalent D_2-filled implosions using the Neutron Temporal Diagnostic (NTD).[32] A laser absorption fraction of $41\% \pm 1\%$ in the 23 kJ implosions was recorded by full aperture backscatter stations (FABS).[33] The recorded bang time and absorption fraction were used to constrain simulations of these implosions.

The recorded yields are presented in Figure 3(a), and the ratio of observed yield to expected yields from 1D HYADES simulations ("yield-over-clean" or YOC) is presented in Figure 3(b). In all CD-shell experiments, the DD-neutron yield is of the order of 10^{10}. This is in reasonable agreement with 1D-simulations, which predict nuclear yield of approximately $2\text{–}3 \times 10^{10}$ from the CD shell in addition to yield from the fuel. D^3He-proton yields are measured above 10^{10} for both pure ^{3}He- and D^3He-filled targets. YOC is shown both including and excluding the CD-shell DD-neutron yield, assuming that the shell yield is the same in all experiments with the same laser energy, and is equal to the total neutron yield from the pure ^{3}He-filled experiments. Both DD-neutron and D^3He-proton YOC values are comparable to those reported for thin-glass exploding pushers filled with similar levels of 50:50 D^3He fuel.[12] The neutron yield from the shell appears to be somewhat better modeled (YOC = 50%) than yield from the gas (YOC = 20%–40%). Recent experiments imploding identical targets with a shorter 0.6 ns laser impulse at the same peak power as the 23 kJ implosions produced comparable results.

Burn-averaged ion temperatures were inferred from the Doppler-broadened line width of DD-neutrons for all experiments, as shown in Figure 4. The measured temperatures agree well with simulations for the pure ^{3}He-filled experiments, and fall between the simulated shell-only and simulated total burn-average ion temperature for the implosions with D_2 fill. As with the yields, there is better agreement between measured and simulated temperatures for experiments where the yield is produced only in the CD. Both of these results are possibly due to the lower burn temperatures and higher average-Z in the remaining shell material, which produces $\sim 20\times$ shorter ion-ion mean-free-paths during burn as compared to the hot, low-Z fuel. The hydrodynamic equations assume short mean-free-paths relative to zone size, and are therefore more valid during burn in the shell than in the fuel.

IV. ANALYSIS

As reported previously,[19] the yield of D^3He-protons from pure ^{3}He-filled targets was essentially identical to the yield from targets filled with a hydroequivalent 50:50 D:^{3}He

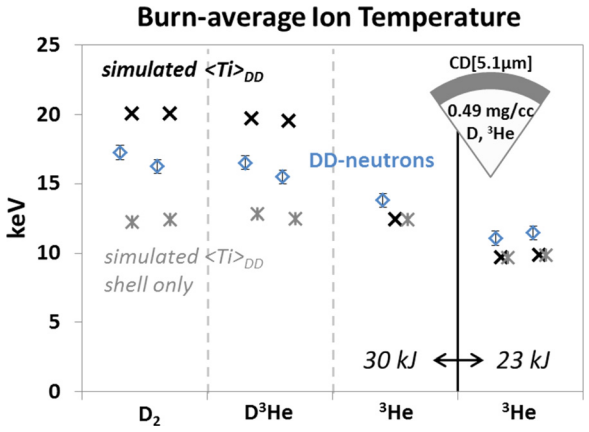

FIG. 4. Nuclear burn-averaged temperatures recorded from the spectral line width of the measured DD-neutrons (open diamonds, blue). DD-neutron burn-averaged ion temperatures predicted from 1D-HYADES simulations are shown for the total experiment (x, black) and for the shell only (stars, grey).

mixture and imploded with identical laser conditions. It has been conclusively shown that the observed D^3He-proton yields in the pure ^3He implosions are the product of fuel-shell mix and that this mix is not hydrodynamic in nature.

A. Nuclear yields

The application of analytical models of yield production as a function of mix and deuterium fraction to the data was attempted, as described in the Appendix. Such analytical models did not converge to consistent solutions. One source of this inconsistency is apparent in the DD-neutron yield-over-clean for the fuel shown in Fig. 3, which is less in the pure D_2 implosions (25%) than in the 50:50 implosions (35%). The pure deuterium fuel appears to be underperforming, in terms of both DD-neutron yield and temperature, compared to the 50:50 D^3He fuel. Such non-hydroequivalent performance has been observed in the compression yield of ablatively driven D^3He targets, but with an opposite trend, such that 50:50 D^3He-filled implosions underperformed relative to hydroequivalent D_2 fills.[23] This data underscores the value of a more thorough study of the hydrodynamic equivalence of shock-driven implosions in the future. One possible explanation is that kinetic effects dominate the evolution of these implosions prior to and during burn, such that models based on hydrodynamic equivalence are inappropriate for explaining the yield trends even in the D_2 and 50:50 D^3He cases.

A simulation technique incorporating RIK models in a 1D fluid-based radiation-hydrodynamic code was applied to these experiments. The RIK models represent the effects of kinetic transport of ion mass (ion diffusion) and energy (ion thermal conduction), as well as the reduction in fusion reactivity due to loss of energetic Maxwellian-tail ions (Knudsen-layer depletion); each kinetic model includes a single free parameter.[21,34] These model parameters were calibrated to a subset (four shots) and the entire set (eight shots) of thin glass-shell D^3He implosion data with comparable fuel densities, as described in Ref. 12. Both calibrations were applied to simulations of the experiments discussed here, and the average and variance of these results is presented in Table I, along with the observed values for those shots. The RIK models capture the trends of the observed yields and ion temperatures much more accurately than the clean simulations (Figs. 3 and 4), and produced 60% of the observed D^3He-proton yield for the pure ^3He implosion (#65278).

The effects of each of the three RIK models on the simulations is presented in Figure 5, which shows the measured data plotted as a function of deuterium fraction in the fuel, compared to simulations run with the three RIK models turned on sequentially. The "four-shot" calibrated parameters were used for this study. Of the three RIK models, only the ion diffusion model introduces the ion mass transport necessary for generating significant D^3He-proton yield from a pure ^3He implosion. With the ion kinetic parameters turned off (the "clean" simulation in Fig. 5), the D^3He-proton yield from the pure ^3He implosion dropped to $\sim 10^6$.[35] Including ion diffusion in the simulations, the trend of the data is captured for both D^3He-protons and DD-neutrons. It is noteworthy that in addition to reproducing the observed high D^3He-proton yields for pure ^3He fuels ($f_D = 0$), the ion diffusion model also reproduces the observed low DD-neutron yields for pure deuterium fuels ($f_D = 1$). These features strongly support the ion diffusive explanation of the observed data. Knudsen-layer reactivity reduction and ion thermal conduction both reduce the yields, better capturing the absolute yields measured; reactivity reduction is predicted to be the stronger of these two effects.

The necessary conditions for strong ion diffusion at the fuel-shell interface do not hold in ignition experiments generally, where the diffusion coefficient $D \propto T^{5/2}/n_i$ remains low throughout the experiment due to either low temperature (prior to compression) or high density (during compression).[8] However, ion diffusion has not previously been studied in high-energy-density experiments. Modifications to the shock profile due to differential ion species diffusion could result in changes to the fuel adiabat, altering the initial conditions for compression and burn.[36] This work will contribute to the calibration of ion diffusion models, such as the

TABLE I. Comparison of observed yields and temperatures with 1D fluid-based simulations including RIK models. For the RIK simulations, two sets of model calibration parameters were applied and the results were averaged; the uncertainty indicates the variation between the two sets of parameters.

		DD-neutrons ($\times 10^{10}$)		D^3He-protons ($\times 10^{10}$)		$\langle T_i \rangle_{DD}$ (keV)	
Shot	Fuel	Observed	RIK	Observed	RIK	Observed	RIK
65273	D_2	7.4 ± 0.7	10 ± 4	—	—	16.3 ± 0.5	14.6 ± 1.0
65275	D^3He	3.7 ± 0.4	3.0 ± 0.5	3.8 ± 0.2	2.7 ± 0.1	15.5 ± 0.5	13.2 ± 0.7
65278	^3He	1.5 ± 0.2	1.1 ± 0.1	3.0 ± 0.2	1.8 ± 0.4	13.8 ± 0.5	11.7 ± 0.6

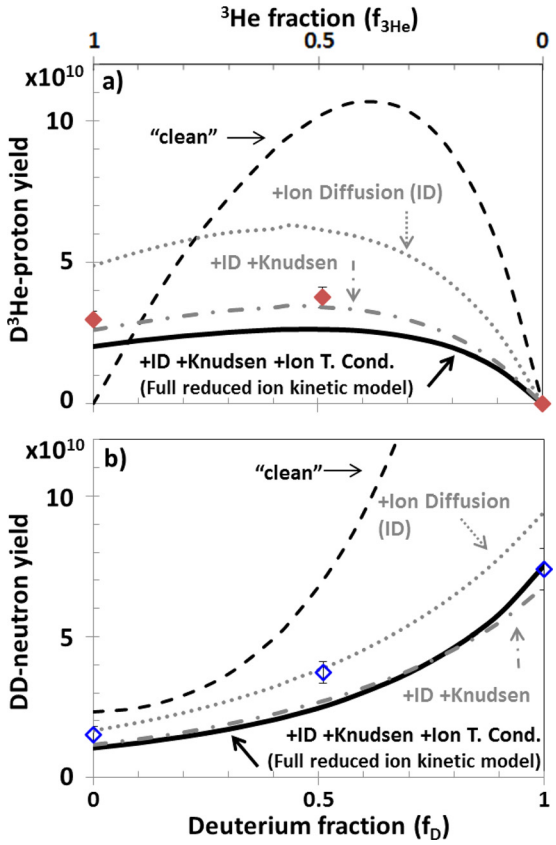

FIG. 5. Measured (a) D^{3}He-proton (red) and (b) DD-neutron (blue) yields as a function of deuterium fraction and ^{3}He fraction ($f_D = 1 - f_{3He}$), compared to a simulation including RIK models (thick line) and "clean" simulations (thin dashed). The RIK simulation shown was calibrated to four D^{3}He-filled thin-glass implosions with comparable fuel density. The individual effects of the three RIK models (ion diffusion, Knudsen reactivity reduction by tail-ion loss, and ion thermal conduction) are evaluated by turning the models on one at a time. Ion diffusion (grey dotted) recaptures the observed trends in the data; Knudsen tail-ion loss (grey dotted-dashed) brings the simulated yields closer to the measured yields. Ion thermal conduction has a smaller effect in these simulations, compared to the other two models.

RIK models discussed above, to further explore the impact of such effects on ignition experiments.

B. Additional kinetic mechanisms

It has been shown that a non-hydrodynamic mechanism is required to explain the results of these experiments. Ion diffusion has been proposed as one possible explanation, as discussed in Ref. 19 and above. Between shell burn-through (~500 ps) and shock bang time (~700 ps), the temperature of the plasma at the fuel-shell interface increases by over a factor of 10 while the density drops, increasing the rate of diffusion dramatically. In simulations including a model of ion diffusion, an approximately 10 μm wide mix region forms prior to shock bang time, which upon reshock generates yields comparable to those observed. However, the initial promise of this ion diffusion model does not rule out the possibility that other kinetic mechanisms may play an important role in these experiments. Several other kinetic mechanisms have been investigated to determine the possible contributors to the observed results.

1. Shock acceleration of deuterons

A mechanism mediated by electric fields at the shock front has been investigated as a possible contributor to the enhanced D^{3}He-proton yield observed in these experiments. Strong electric fields in the shock front[37] will accelerate a population of fast, directional deuterons ahead of the shock. This shock reflection mechanism is similar to the shock unloading or vaporization at a material-gas interface in weak-shock scenarios,[38] and has been studied previously in simulated collisionless[39,40] and collisional shocks.[41] Recent work using fully kinetic simulations of shocks breaking out across fuel-shell interfaces has shown that, in some cases, this mechanism is capable of introducing significant mix of light shell ions into the fuel.[10]

Strong local electric fields E(x) of order 10^9 V/m have been observed near shock fronts in ICF implosions using proton deflectometry.[37,42] These fields generate an electric potential barrier $\Phi = -\int_0^x E(x)dx$, which will reflect deuterons lacking sufficient kinetic energy to surmount it. Electron diffusion across the shock front is expected to dominate electric field generation in these experiments, producing potentials on the order of the post-shock electron temperature, $\Phi \approx T_e/e$.[43] The electron pressure gradient will be used in these calculations to infer local electric field $E(x) = -\nabla P_e/n_e e$, for comparison of the appropriate scale for Φ, although it is approximately an order of magnitude weaker than the expected source from electron diffusion. This difference is a consequence of the shock not being in a steady state due to continuing laser drive.

The fraction of deuterons accelerated is most readily assessed in the reference frame of the shock front. In this frame, inflowing deuterons have velocity $v_x = (\vec{u}_{shock} + \vec{v}_{th})|_x$. Reflected deuterons will satisfy the condition $0 < v_x < \sqrt{2ZE\Phi/m}$, or translating back into the lab frame, $-u_{shock} < v_x < \sqrt{2ZE\Phi/m} - u_{shock}$. Integrating the distribution function over this range of velocities gives the fraction of deuterons that will be accelerated by the shock. For a Maxwell-Boltzmann distribution, this is given by

$$f_{acc} = \frac{1}{2}\left[\mathrm{Erf}\left(\frac{\sqrt{2ZE\Phi/m} - u_{shock}}{v_{th}}\right) - \mathrm{Erf}\left(-\frac{u_{shock}}{v_{th}}\right)\right], \quad (1)$$

where $v_{th} = \sqrt{2T/m}$ is the thermal velocity of deuterons upstream of the shock front. For a given v_{th}, the accelerated fraction is maximized when $ZE\Phi = 2mu_{shock}^2$, and falls off rapidly for $ZE\Phi < mu_{shock}^2/2$. In general, the accelerated fraction will be larger when v_{th} is small compared to the terms in the numerator, though the maximum accelerated fraction is above 80% when v_{th} equals the shock velocity.

It is important to note that this formalism neglects collisions of the reflected deuterons within the shock front. Such collisions have been shown to inhibit reflection of deuterons with short mean-free-paths, reducing the reflected fraction.[10] However, the large gradients present at the shock front and the dynamic nature of the reflection effect complicate a full collisional estimate. This derivation provides an upper bound for the reflected population, and a worst-case scenario in terms of the expected mix.

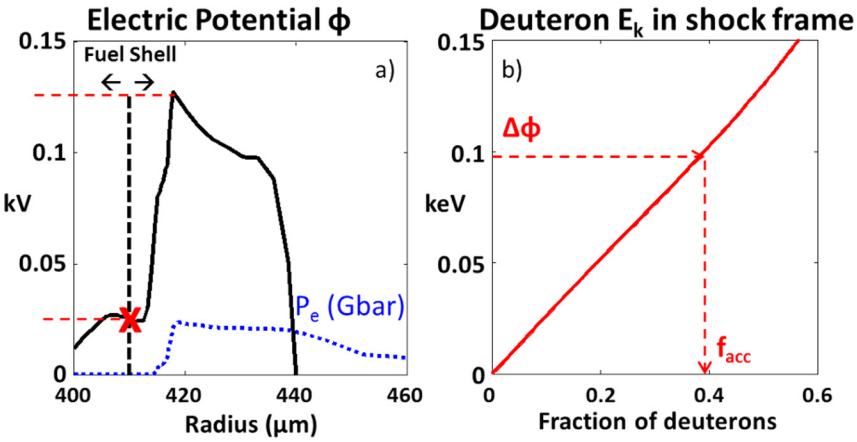

FIG. 6. (a) Radial lineout of electric potential $\Phi_{\nabla Pe}$ inferred from 1D-radiation-hydrodynamic simulations, near shock-breakout from the shell into the ^{3}He fuel (t = 270 ps). The plasma in front of the shock (red x) has $T \sim 30$ eV and $n_i \sim 10^{21}$. (b) The fraction of deuterons in front of the shock below a given kinetic energy in the shock frame. Comparing this curve to the potential jump at the shock front (dashed red line) shows that a large fraction of deuterons (>30%) will be "reflected" by the shock and launched into the ^{3}He fuel at approximately twice the shock velocity.

Figure 6 shows the plasma ∇P_e-induced electric potential near the time of shock breakout (270 ps) as calculated from 1D HYADES simulations. At this time, $u_{shock} \approx 115\,\mu$m/ns, $\Phi_{\nabla Pe} \approx 0.1$ kV, $\Phi_{Te} \approx 1.6$ kV. The CD plasma in front of the shock is not fully ionized, with $T_e = T_i \approx 30$ eV, $\langle Z \rangle = 1.5$, and ion density of order 10^{21} cm^{-3}.[44] Applying Eq. (1) to this plasma determines that 36% of the pre-shock deuterons are expected to be accelerated by the potential $\Phi_{\nabla Pe}$, as shown in Figure 6. If the potential scales with the much stronger Φ_{Te} as is expected, then 99% of the pre-shock deuterons will be accelerated by this process.

Shock-accelerated deuterons within a mean-free-path of the fuel-shell interface will stream into the ^{3}He gas. Using a model for scattering in strongly coupled plasmas,[45] $\lambda_{MFP} \approx 3\,\mu$m for deuterons traveling at $2u_{shock}$ through the plasma conditions described above. The expected number of deuterons kinetically mixed into the ^{3}He gas is calculated to be $f_{acc} n_D (4\pi R^2) \lambda_{MFP} \approx 3 \times 10^{15}$, assuming 99% reflection. This is approximately 10% the number of ^{3}He atoms in the fuel.

The mean-free-path for these reflected deuterons in the unshocked ^{3}He plasma is approximately 3 μm. This value is similar to the mean-free-path in the CD plasma because the ^{3}He is pre-compressed by the blowdown of preheated CD material. Once inside the ^{3}He, the deuterons will thermalize and move with the fluid throughout the implosion and burn. Artificially introducing 3×10^{15} deuterons into the outermost 3 μm of the ^{3}He fuel in the simulations produces of order 10^{10} D^{3}He-protons, comparable to what is observed. It is worth noting that the shock will continue reflecting deuterons as it passes through the fuel. In the latter scenario, the shock may carry a population of "surfing" deuterons much deeper into the fuel. If some or all of these deuterons later thermalize volumetrically in the fuel, they will provide a uniform atomic mix background for fusion production at shock bang-time. Such behavior could be diagnosed by imaging the region of fusion burn in the experiment.[46] The signature of volumetric burn is predicted to be measurably different from the ion-diffusion mechanism, which is expected to produce fusion yield in a narrow region near the fuel-shell interface.

Baro-,[8] electro-,[9] and thermo-diffusion[47] at the shock front has recently been studied as a mechanism driving species separation in mixed plasmas. In a CD plasma which has not been fully ionized, pressure, electric-field, and thermal terms are all expected to push deuterium ahead of the shock.[47] If deuterium is pushed ahead of the shock front by these diffusion mechanisms, they would increase the population of deuterium available for acceleration and mixture at the fuel-shell interface.

An upper bound for the amount of shock accelerated deuterium has been calculated to be comparable to the value required to explain the data. Further theory and kinetic simulations are required to estimate how much the accelerated deuteron fraction is reduced from this prediction due to collisionality in the shock front, and to understand the extent to which this mechanism occurs in ignition experiments. However, it is clear from these calculations that the strong electric field at the shock front can significantly modify the shock dynamics in these implosions and must be considered.

2. Beam-target fusion

Another mechanism which has been proposed to account for this data is beam-target fusion, wherein a population of directed ions encounters a plasma containing a reactant species. Several mechanisms may create such a non-thermal population of radially streaming ions in these experiments, including shock acceleration as discussed in Sec. IV B 1, insufficient thermalization times for the shocked fuel, and loss of confinement of ions on the thermal high-energy tail due to long mean-free-paths.[34] It will be shown that none of these beam-target mechanisms are expected to produce significant fusion yield in these experiments.

a. Shock acceleration. The shock acceleration mechanism described previously has been shown to generate a population of deuterons streaming into the ^{3}He fuel. However this population is not sufficiently energetic to generate significant beam-target fusion. In any beam-target scenario, the fusion probability depends very strongly on the velocity of this directional population, as center of mass energy E_{CM} of the collision between ions 1 and 2 is $E_{CM} = E_1 m_2/(m_1 + m_2) \propto v_1^2$ if species 2 is at rest, and the D-^{3}He fusion cross section is roughly proportional to E_{CM}^3 for $E_{CM} < 150$ keV.[48] At twice the shock velocity, the streaming deuterons carry a kinetic energy of only 0.14 keV; and the

collisional center-of-mass energy for these deuterons on static ^{3}He is $E_{CM} = 0.6E_D \approx 0.08$ keV. This energy is low enough that it is unlikely that any of the accelerated deuterons will fuse with a ^{3}He ion at this stage.

Reflection of ^{3}He ions by the rebounding shock after shock convergence will produce a population of much more energetic ions, as the shock strength and shock velocity increase significantly with spherical convergence. However, the shock acceleration mechanism is less efficient at shock rebound than at shock breakout. The electric field strength due to the electron pressure gradient and electron temperature sources are roughly comparable at shock rebound ($\sim$1 keV). Electron-ion thermal equilibration is of order 10 ns at shock rebound, which is long compared to dynamical timescales: for example, the fusion burn duration was measured to have a full-width at half maximum of 180 ps. The shock thermal energy is not transferred efficiently to the electrons and electron temperature remains in the range of 3–5 keV. On the basis of Eq. (1), it is expected that the fraction of shock-accelerated ^{3}He ions is less than 1%.

An approximate fusion yield for this reflected population was calculated based on 1D HYADES simulations. Profiles of density, temperature, and plasma flow velocity in the CD shell and a model of plasma stopping power[49] were used to determine the energy as a function of distance for a ^{3}He ion with known initial energy escaping the implosion. The collisional center-of-mass energy of the ^{3}He ion with thermal deuterons was calculated for each zone, taking into account the background plasma flow, and a parametrized D-^{3}He fusion cross-section model[48] was used to determine the total fusion probability. Assuming 1% of ^{3}He ions are reflected at the shock front and travel at twice the rebound shock velocity, the beam-target fusion generated is approximately 1.4×10^9, which is an order of magnitude below the observed yields.

Simple energetics arguments suggest that explaining the results with a shock-reflected ^{3}He population is implausible. A ^{3}He ion traveling at this speed contains 168 keV of kinetic energy. If 20% of the ^{3}He ions were reflected, as would be required to explain the observed yield using this mechanism alone, this population would contain 160 J of kinetic energy, which is approximately the total energy delivered to the ^{3}He plasma by the implosion. Even a fraction of this number would begin to significantly drain the energy of the rebound shock, thereby inhibiting further reflection.

b. Non-thermalized shock energy. If upon shock convergence the ^{3}He plasma is not fully thermalized due to long thermalization times, the radially inward-directed ^{3}He fluid might directly produce a population of radially outward-directed ^{3}He ions after convergence. At shock convergence, the calculated ion-ion thermalization times are in excess of 1 ns, which is long compared to dynamical timescales ($\sim$200 ps). Such a population would be expected to maintain velocity v_{3He} equal to or less than the fluid velocity behind the incoming shock, v_1. In simulations of these experiments, the mass-average incoming fluid velocity $\langle v_1 \rangle = 1100\,\mu$m/ns just prior to shock convergence, which is approximately 70% of the rebound shock velocity. The center-of-mass energy would thus be $\sim$0.14$\times$ that of the shock-accelerated ^{3}He considered above, and the fusion reactivity reduced by a factor of approximately 400. The predicted yield from this mechanism was calculated using the same technique as was used for the shock acceleration mechanism. Assuming all ^{3}He are radially directed outward at $\langle v_1 \rangle$, the predicted yield due to non-thermalized, shocked ^{3}He is less than 1×10^8, over two orders of magnitude lower than the observed yields.

c. Long mean-free-paths. Loss of ion confinement due to long ion-ion mean-free-paths[34] provides another kinetic source of radially directed, high-energy ^{3}He ions in these experiments. Given the low density and high temperatures produced in the central plasma, the mean-free-path of ^{3}He ions at peak compression are expected to be approximately equal to the radius of the shell at peak convergence. In this scenario, kinetic effects have been shown to play a strong role in the dynamics of fusion yield production.[12] In particular, the mean-free-path of the energetic ions which dominate fusion production is several times longer than the thermal mean-free-path. The energetic ^{3}He ions are free to stream into the remaining CD plasma, where fusion reactions can occur with a probability determined by the collisional center-of-mass energy as the ions slow down.

An upper bound to the total yield generated from this mechanism was calculated by assuming all ^{3}He ions in the plasma are in a thermalized distribution and escape radially into the CD plasma without first slowing on the ^{3}He.[50] The fusion probability was calculated for each initial ion energy as above, and then weighted by the number of ions with that energy in a Maxwell-Boltzmann distribution for the selected ion temperature. This calculation produces approximately 6×10^9 D^{3}He reactions, a factor of 5 less than the yields observed.

Although it has been shown that these mechanisms are not likely to be strong enough to play a significant role in the experiments, it is worth considering what experimental signatures might be used to differentiate between yields produced by various mechanisms. One signature of a beam-target mechanism would be broadening of the fusion product spectral lines. For thermal plasmas, the fusion spectral line width is Doppler broadened by center-of-mass velocity of the reacting ions, and is roughly proportional to the square root of the ion temperature.[51,52] This effect is exacerbated in the "spherical beam-target" scenario described above, as the center-of-mass velocity of each reaction is radially directed outward from the plasma. Following Ref. 52, the observed particle energy of a fusion product from a reaction with center-of-mass velocity V_{CM} is

$$E_1' = \frac{1}{2} m_1' V_{CM}^2 + \frac{m_2'}{m_1' + m_2'}(Q + K) + |V_{CM}| \cos\theta \sqrt{\frac{2m_1' m_2'}{m_1' + m_2'}(Q + K)}, \quad (2)$$

where m' are the fusion product masses, Q is the energy released by the fusion reaction, K is the total kinetic energy

in the center-of-mass system ($K \ll Q$), and θ is the angle between the center-of-mass velocity and the direction of the nuclear product. The broadening of the spectral peak is governed by the (directional) $\cos\theta$ term. In a thermal plasma, V_{CM-th} will have a roughly normal distribution and θ will be independent of where the reaction occurs in the plasma. In the beam-target reactions described above, $|V_{CM-beam}|$ is roughly constant and θ is correlated to reaction location: for the "near" side of the implosion, $\theta = 0$, whereas for the "far" side, $\theta = \pi$. The fusion product energy is thus a function of angle, $E'(\theta) = E'_0 + E'_{beam}\cos\theta$, where $E'_{beam} = V_{CM-beam}\sqrt{Qm'_1m'_2/(m'_1+m'_2)}$. Taking the 2nd moment of $E(\theta)$, and rewriting $V_{CM-beam}$ in terms of the beam-particle energy $E_1 = (m_1+m_2)^2V^2_{CM-beam}/2m_1$, the spectral width of the fusion products is obtained as

$$\sigma^2_{beam} = \frac{4}{3}\frac{m'_1m'_2}{(m'_1+m'_2)}\frac{m_1}{(m_1+m_2)^2}(Q+K)E_1. \qquad (3)$$

This derivation is identical to the thermal case, except with $E_1 \propto V^2_{CM-beam}$ in lieu of $\langle V^2_{CM-th}\rangle$. In the case of energetic ^{3}He fusing with a static shell of D, the formula for proton spectral width may be simplified to $\sigma^2_{beam} \approx E_1(2340\,\text{keV})$. By comparison with the well-known relationship for D^{3}He protons from a thermal fusion source, $\sigma^2_{th} \approx T_i(5880\,\text{keV})$, it is clear that a radially symmetric population with energy E_1 in excess of 2.5 times the thermal energy will produce a wider spectral line than the thermal ions.[51] For the calculations described above, ^{3}He ions at the shock velocity carry 40 keV, and would generate a proton line width ($\sigma \approx 300$ keV) equivalent to 16 keV thermal temperature. Such temperatures are reasonably achieved in these and similar experiments, and as such could not be discriminated using this technique. However shock-accelerated ^{3}He ions carrying 160 keV would generate a proton line width ($\sigma \approx 600$ keV) equivalent to 64 keV, which would be unreasonably high and represent a measurable signature of this effect.

V. CONCLUSION

Several kinetic mechanisms were considered as possible contributing factors to mix in implosions of thin CD-shells filled with pure ^{3}He, which have previously been shown to produce yield equivalent to that from 50:50 D^{3}He fill due to a non-hydrodynamic mix mechanism. Fluid simulations including reduced ion kinetic models match the observed trends of yield and ion temperature in these implosions, strengthening the case for ion diffusion. Of the other models considered, electric field acceleration of the deuterium ions at the shock front is predicted to have the strongest effect. As shocks break out across the fuel-shell interface, a substantial fraction of deuterons near the interface are accelerated to approximately twice the shock speed, and deuterons within a mean-free path of the interface are free to stream into the ^{3}He plasma. An upper bound for the number of deuterons accelerated is calculated to be comparable to the number required to explain the yield results. Several "beam-target" fusion mechanisms were considered, but all are predicted to produce yield at least an order of magnitude below what was observed. Fully kinetic simulations of such implosions, especially of shock breakout across the fuel-shell interface, will be highly informative in terms of better understanding the detailed mechanics of kinetic mix in these implosions, and their application to other experiments of interest, such as CH/DT interfaces in ignition experiments. Upcoming imaging of the nuclear burn region will provide additional data for further determining the dominant mechanism of non-hydrodynamic mix in these experiments.

ACKNOWLEDGMENTS

The authors thank R. Frankel and E. Doeg for contributing to the processing of CR-39 data used in this work, as well as the OMEGA operations crew for their help in executing these experiments. This work is presented in partial fulfillment of the first author's Ph.D. thesis and supported in part by US DoE (Grant No. DE-NA0001857), FSC (No. 5-24431), NLUF (No. DE-NA0002035), LLE (No. 415935-G), LLNL (No. B597367), and NNSA Stewardship Science Graduate Fellowship (DE-FC52-08NA28752).

APPENDIX: ANALYTICAL YIELD MODEL

An analytical model based on hydroequivalence of the fuels was developed to constrain the amount of mix. The nuclear yields are given by volume and time integrals of the reactive ion species densities and the reactivity, as follows:

$$Y_{DD-n} = \int (n_D^2/2)\langle\sigma v\rangle_{DD}dVdt,$$
$$Y_{D3He-p} = \int n_D n_{3He}\langle\sigma v\rangle_{D^3He}dVdt. \qquad (A1)$$

The hydroequivalence of the different fills implies that the evolution of temperature and mass-density profiles of each experiment are the same to zeroth order. The species densities n_i in Eq. (A1) may be rewritten in terms of mass density ρ, which is identical for all experiments, and the deuterium number fraction f_D, as follows: $n_D = \rho f_D/m_p(3-f_D)$, $n_{3He} = \rho(1-f_D)/m_p(3-f_D)$. Assuming f_D does not evolve within an implosion, it may be removed from the integral, and a scaling of yield versus f_D derived.

Two sources of DD-neutron yield are expected: yield from the deuterium in the initial gas fill and yield from the deuterium in the shell. While the former is expected to follow the hydroequivalent scaling $Y_{DD}(f_D) = Y_{DD}(f_D=1)\,4f_D^2/(3-f_D)^2$,[23] the latter should be approximately constant for the unmixed fuel region in all experiments.

Attempts to constrain a model of the different yield-producing regions to the data based on the dual assumptions of fuel hydroequivalence and perturbative deuterium mix into the fuel did not converge to a consistent solution. A model for the DD-neutron yields was developed by assuming that the yield from the CD-shell is equal in all experiments, the yield from the fuel scales as n_D^2, and the initially hydroequivalent fuels were perturbed by an equal amount of shell-deuterium mix in all experiments. The deuterium density is

modeled as $n_D \rightarrow n_D + n_{mix} = (\rho/m_p)[f_D/(3-f_D) + f_{mix}/2]$. This model has three variables: shell yield, fuel yield from a "clean" D_2 implosion, and mix fraction. Using the DD-neutron data from the experiments presented in Fig. 3, for which $f_D = 0$, 0.5, and 1, to solve this system of equations, the model does not converge to a reasonable solution: the shell yield is required to be consistent with 0, while mix generates the majority of yield for all deuterium fractions. Such a strongly mixed scenario violates the condition of hydroequivalence. Additionally, this scenario is inconsistent with burn-average ion temperature data (Fig. 4): the temperatures from the pure ^{3}He implosions are in good agreement with simulations, which predict shell-yield only, whereas a higher burn-average temperature would be expected if volumetrically mixed deuterium were dominant.

As discussed in Sec. IV A, the assumption of hydroequivalent yield performance in these implosions is likely to be invalidated by the kinetic nature of the plasmas. The much better agreement with the observed yield and temperature trends produced by simulations including reduced ion kinetic models, as compared to "clean" hydrodynamic simulations (see Figure 5), supports this finding.

[1]J. Lindl, Phys. Plasmas **2**, 3933 (1995).
[2]Y. Aglitskiy, A. L. Velikovich, M. Karasik, V. Serlin, C. J. Pawley, A. J. Schmitt, S. P. Obenschain, A. N. Mostovych, J. H. Gardner, and N. Metzler, Phys. Rev. Lett. **87**, 265001 (2001).
[3]V. A. Smalyuk, S. X. Hu, J. D. Hager, J. A. Delettrez, D. D. Meyerhofer, T. C. Sangster, and D. Schvarts, Phys. Rev. Lett. **103**, 105001 (2009).
[4]S. E. Bodner, Phys. Rev. Lett. **33**, 761 (1974).
[5]M. J. de C. Henshaw, G. J. Pert, and D. L. Youngs, Plasma Phys. Control Fusion **29**, 405 (1987).
[6]K. O. Mikaelian, Phys. Fluids **6**, 1943 (1994).
[7]A. L. Velikovich, A. J. Schmitt, J. H. Gardner, and N. Metzler, Phys. Plasmas **8**, 592 (2001).
[8]P. Amendt, C. Bellei, and S. Wilks, Phys. Rev. Lett. **109**, 075002 (2012).
[9]G. Kagan and X.-Z. Tang, Phys. Plasmas **19**, 082709 (2012).
[10]C. Bellei, H. Rinderknecht, M. Rosenberg, A. Zylstra, H. Sio, C. Li, R. Petrasso, S. Wilks, and P. Amendt, Phys. Plasmas **21**, 056310 (2014).
[11]C. Bayer, M. Bernard, D. Billon, M. Decroisette, D. Galmiche, D. Juraszek, J. Launspach, D. Meynial, and B. Sitt, Nucl. Fusion **24**, 573 (1984).
[12]M. J. Rosenberg, H. G. Rinderknecht, N. M. Hoffman, P. A. Amendt, S. Atzeni, A. B. Zylstra, C. K. Li, F. H. Seguin, H. Sio, M. G. Johnson, J. A. Frenje, R. D. Petrasso, V. Y. Glebov, C. Stoeckl, W. Seka, F. J. Marshall, J. A. Delettrez, T. C. Sangster, R. Betti, V. N. Goncharov, D. D. Meyerhofer, S. Skupsky, C. Bellei, J. Pino, S. C. Wilks, G. Kagan, K. Molvig, and A. Nikroo, Phys. Rev. Lett. **112**, 185001 (2014).
[13]R. D. Petrasso, J. A. Frenje, C. K. Li, F. H. Séguin, J. R. Rygg, B. E. Schwartz, S. Kurebayashi, P. B. Radha, C. Stoeckl, J. M. Soures, J. Delettrez, V. Y. Glebov, D. D. Meyerhofer, and T. C. Sangster, Phys. Rev. Lett. **90**, 095002 (2003).
[14]J. R. Rygg, J. A. Frenje, C. Li, F. Séguin, R. D. Petrasso, V. Y. Glebov, D. Meyerhofer, T. Sangster, and C. Stoeckl, Phys. Rev. Lett. **98**, 215002 (2007).
[15]D. C. Wilson, P. S. Ebey, T. C. Sangster, W. T. Schamyda, V. Y. Glebov, and R. A. Lerche, Phys. Plasmas **18**, 112707 (2011).
[16]V. A. Smalyuk, R. E. Tipton, J. E. Pino, D. T. Casey, G. P. Grim, B. A. Remington, D. P. Rowley, S. V. Weber, M. Barrios, L. R. Benedetti, D. L. Bleuel, D. K. Bradley, J. A. Caggiano, D. A. Callahan, C. J. Cerjan, D. S. Clark, D. H. Edgell, M. J. Edwards, J. A. Frenje, M. Gatu-Johnson, V. Y. Glebov, S. Glenn, S. W. Haan, A. Hamza, R. Hatarik, W. W. Hsing, N. Izumi, S. Khan, J. D. Kilkenny, J. Kline, J. Knauer, O. L. Landen, T. Ma, J. M. McNaney, M. Mintz, A. Moore, A. Nikroo, A. Pak, T. Parham, R. Petrasso, D. B. Sayre, M. B. Schneider, R. Tommasini, R. P. Town, K. Widmann, D. C. Wilson, and C. B. Yeamans, Phys. Rev. Lett. **112**, 025002 (2014).
[17]V. A. Smalyuk, M. Barrios, J. A. Caggiano, D. T. Casey, C. J. Cerjan, D. S. Clark, M. J. Edwards, J. A. Frenje, M. Gatu-Johnson, V. Y. Glebov, G. Grim, S. W. Haan, B. A. Hammel, A. Hamza, D. E. Hoover, W. W. Hsing, O. Hurricane, J. D. Kilkenny, J. L. Kline, J. P. Knauer, J. Kroll, O. L. Landen, J. D. Lindl, T. Ma, J. M. McNaney, M. Mintz, A. Moore, A. Nikroo, T. Parham, J. L. Peterson, R. Petrasso, L. Pickworth, J. E. Pino, K. Raman, S. P. Regan, B. A. Remington, H. F. Robey, D. P. Rowley, D. B. Sayre, R. E. Tipton, S. V. Weber, K. Widmann, D. C. Wilson, and C. B. Yeamans, Phys. Plasmas **21**, 056301 (2014).
[18]D. T. Casey, V. A. Smalyuk, R. E. Tipton, J. E. Pino, G. P. Grim, B. A. Remington, D. P. Rowley, S. V. Weber, M. Barrios, R. Benedetti, D. L. Bleuel, E. J. Bond, D. K. Bradley, J. A. Caggiano, D. A. Callahan, C. J. Cerjan, D. H. Edgell, M. J. Edwards, D. Fittinghoff, J. A. Frenje, M. Gatu-Johnson, V. Y. Glebov, S. Glenn, N. Guler, S. W. Haan, A. Hamza, R. Hatarik, D. Hoover, W. W. Hsing, N. Izumi, P. Kervin, S. Khan, J. D. Kilkenny, J. Kline, J. Knauer, O. L. Landen, T. Ma, J. M. McNaney, M. Mintz, A. Moore, A. Nikroo, A. Pak, T. Parham, R. Petrasso, H. G. Rinderknecht, D. B. Sayre, M. Schneider, R. Tommasini, R. P. Town, K. Widmann, D. C. Wilson, and C. B. Yeamans, "Development of the CD Symcap platform to study gas-shell mix in implosions at the National Ignition Facility," Phys. Plasmas (submitted).
[19]H. G. Rinderknecht, H. Sio, C. Li, A. Zylstra, M. Rosenberg, P. Amendt, J. Delettrez, C. Bellei, J. A. Frenje, M. G. Johnson, F. Séguin, R. D. Petrasso, R. Betti, V. Y. Glebov, D. Meyerhofer, T. Sangster, C. Stoeckl, S. Wilks, A. Greenwood, and A. Nikroo, Phys. Rev. Lett. **112**, 135001 (2014).
[20]S. W. Haan, J. D. Lindl, D. A. Callahan, D. S. Clark, J. D. Salmonson, B. A. Hammel, L. J. Atherton, R. C. Cook, M. J. Edwards, S. Glenzer, A. V. Hamza, S. P. Hatchett, M. C. Herrmann, D. E. Hinkel, D. D. Ho, H. Huang, O. S. Jones, J. Kline, G. Kyrala, O. L. Landen, B. J. MacGowan, M. M. Marinak, D. D. Meyerhofer, J. L. Milovich, K. A. Moreno, E. I. Moses, D. H. Munro, A. Nikroo, R. E. Olson, K. Peterson, S. M. Pollaine, J. E. Ralph, H. F. Robey, B. K. Spears, P. T. Springer, L. J. Suter, C. A. Thomas, R. P. Town, R. Vesey, S. V. Weber, H. L. Wilkens, and D. C. Wilson, Phys. Plasmas **18**, 051001 (2011).
[21]N. M. Hoffman, G. B. Zimmerman, K. Molvig, E. Dodd, B. Albright, A. Simakov, H. Herrmann, Y. Kim, M. Rosenberg, H. Rinderknecht, H. Sio, A. Zylstra, M. G. Johnson, F. Séguin, J. Frenje, C. Li, R. Petrasso, C. Horsfield, M. Rubery, V. Glebov, C. Stoeckl, W. Seka, and C. Sangster, "Reduced models for the ion-kinetic regime in inertial-confinement-fusion capsule implosions," Phys. Plasmas (to be submitted).
[22]T. R. Boehly, D. L. Brown, R. S. Craxton, R. L. Keck, J. P. Knauer, J. H. Kelly, T. J. Kessler, S. Kumpan, S. Loucks, S. Letzring, F. Marshall, R. L. McCrory, S. Morse, W. Seka, J. Soures, and C. Verdon, Opt. Commun. **133**, 495 (1997).
[23]J. R. Rygg, J. A. Frenje, C. K. Li, F. H. Séguin, R. D. Petrasso, J. A. Delettrez, V. Y. Glebov, V. N. Goncharov, D. Meyerhofer, S. Regan, T. Sangster, and C. Stoekcl, Phys. Plasmas **13**, 052702 (2006).
[24]Small differences due to changes in the fuel radiative loss (a function of average fuel charge-state $\langle Z \rangle$) are predicted to change the yields by $\leq$10%.
[25]S. Skupsky and R. S. Craxton, Phys. Plasmas **6**, 2157 (1999).
[26]Y. Lin, T. J. Kessler, and G. N. Lawrence, Opt. Lett. **21**, 1703 (1996).
[27]J. T. Larsen and S. M. Lane, J. Quant. Spectrosc. Radiat. Transfer **51**, 179 (1994).
[28]S. Atzeni and J. Meyer-Ter-Vehn, *The Physics of Inertial Fusion: Beam Plasma Interaction, Hydrodynamics, Hot Dense Matter*, International Series of Monographs on Physics (Oxford University Press, 2004).
[29]S. W. Haan, Phys. Rev. A **39**, 5812 (1989).
[30]F. H. Séguin, J. A. Frenje, C. K. Li, D. G. Hicks, S. Kurebayashi, J. R. Rygg, B.-E. Schwartz, R. D. Petrasso, S. Roberts, J. M. Soures, D. D. Meyerhofer, T. C. Sangster, J. P. Knauer, C. Sorce, V. Y. Glebov, C. Stoeckl, T. W. Phillips, R. J. Leeper, K. Fletcher, and S. Padalino, Rev. Sci. Inst. **74**, 975 (2003).
[31]V. Y. Glebov, C. Stoeckl, T. Sangster, S. Roberts, G. Schmid, R. Lerche, and M. Moran, Rev. Sci. Instrum. **75**, 3559 (2004).
[32]R. A. Lerche, D. W. Phillion, and G. L. Tietbohl, Rev. Sci. Instrum. **66**, 933 (1995).
[33]W. Seka, H. A. Baldis, J. Fuchs, S. P. Regan, D. D. Meyerhofer, C. Stoeckl, B. Yaakobi, R. S. Craxton, and R. W. Short, Phys. Rev. Lett. **89**, 175002 (2002).
[34]K. Molvig, N. M. Hoffman, B. J. Albright, E. M. Nelson, and R. B. Webster, Phys. Rev. Lett. **109**, 095001 (2012).
[35]Produced by in-flight reactions in the CD plasma.

[36]P. Amendt, C. Bellei, C. K. Li, and R. D. Petrasso, "Shock-driven resistive heating in mixed species thermonuclear fuels," Phys. Rev. Lett. (submitted).
[37]C. K. Li, F. H. Séguin, J. R. Rygg, J. A. Frenje, M. Manuel, R. D. Petrasso, R. Betti, J. Delettrez, J. P. Knauer, F. Marshall, D. D. Meyerhofer, D. Shvarts, V. A. Smalyuk, C. Stoeckl, O. L. Landen, R. P. J. Town, C. A. Back, and J. D. Kilkenny, Phys. Rev. Lett. **100**, 225001 (2008).
[38]Y. B. Zel'dovich and Y. P. Raizer, in *Physics of Shock Waves and High-Temperature Hydrodynamic Phenomena*, edited by W. D. Hayes and R. F. Probstein (Dover Publications, 2002).
[39]D. W. Forslund and C. R. Shonk, Phys. Rev. Lett. **25**, 1699 (1970).
[40]L. O. Silva, M. Marti, J. Davies, R. Fonseca, C. Ren, F. Tsung, and W. B. Mori, Phys. Rev. Lett. **92**, 015002 (2004).
[41]F. Vidal, J. P. Matte, M. Casanova, and O. Larroche, Phys. Fluids B **5**, 3182 (1993).
[42]J. R. Rygg, F. H. Séguin, C. K. Li, J. A. Frenje, M. J.-E. Manuel, R. D. Petrasso, R. Betti, J. A. Delettrez, O. V. Gotchev, J. P. Knauer, D. D. Meyerhofer, F. J. Marshall, C. Stoeckl, and W. Theobald, Science **319**, 1223 (2008).
[43]P. A. Amendt, J. L. Milovich, S. C. Wilks, C. K. Li, R. D. Petrasso, and F. H. Séguin, Plasma Phys. Control Fusion **51**, 124048 (2009).
[44]This model includes the predicted effect of x-ray preheat of the CD, which both heats the inner CD layer and causes it to "blow down" by 20 μm prior to shock breakout.
[45]S. D. Baalrud, Phys. Plasmas **19**, 030701 (2012).
[46]F. Seguin, J. L. DeCiantis, J. A. Frenje, S. Kurebayashi, C. K. Li, J. R. Rygg, C. Chen, V. Berube, B. E. Schwartz, R. D. Petrasso, V. A. Smalyuk, F. J. Marshall, J. P. Knauer, J. A. Delettrez, P. W. McKenty, D. D. Meyerhofer, S. Roberts, T. C. Sangster, K. Mikaelian, and H. S. Park, Rev. Sci. Instrum. **75**, 3520 (2004).
[47]G. Kagan and X.-Z. Tang, "Thermo-diffusion in inertially confined plasmas," Phys. Lett. A **378**, 1531–1535 (2014); e-print arXiv:1310.8227.
[48]H.-S. Bosch and G. M. Hale, Nucl. Fusion **32**, 611 (1992).
[49]C.-K. Li and R. D. Petrasso, Phys. Rev. Lett. **70**, 3059 (1993).
[50]The scenario described is an upper bound, as energy loss by ions escaping during thermalization would prevent such a state from forming. ^{3}He ions are not expected to acquire significantly more energy through collisions than the energy at which $\lambda_{ii} = \mathrm{Rfuel}$, which in this case is $\sim$20 keV: well below the energies expected to dominate fusion reactions.
[51]H. Brysk, Plasma Phys. **15**, 611 (1973).
[52]L. Ballabio, J. Kallne, and G. Gorini, Nucl. Fusion **38**, 1723 (1998).